STEM CELLS AND DEVELOPMENT
Volume 23, Number 5, 2014

DOI: 10.1089/scd.2013.0263

Generation of Highly Purified Neural Stem Cells from Human Adipose-Derived Mesenchymal Stem Cells by *Sox1* Activation

Nianhua Feng,[1] Qin Han,[1] Jing Li,[1] Shihua Wang,[1] Hongling Li,[1] Xinglei Yao,[1] and Robert Chunhua Zhao[1,2]

Neural stem cells (NSCs) are ideal candidates in stem cell-based therapy for neurodegenerative diseases. However, it is unfeasible to get enough quantity of NSCs for clinical application. Generation of NSCs from human adipose-derived mesenchymal stem cells (hAD-MSCs) will provide a solution to this problem. Currently, the differentiation of hAD-MSCs into highly purified NSCs with biological functions is rarely reported. In our study, we established a three-step NSC-inducing protocol, in which hAD-MSCs were induced to generate NSCs with high purity after sequentially cultured in the pre-inducing medium (Step1), the N2B27 medium (Step2), and the N2B27 medium supplement with basic fibroblast growth factor and epidermal growth factor (Step3). These hAD-MSC-derived NSCs (adNSCs) can form neurospheres and highly express *Sox1*, *Pax6*, *Nestin*, and *Vimentin*; the proportion was 96.1%±1.3%, 96.8%±1.7%, 96.2%±1.3%, and 97.2%±2.5%, respectively, as detected by flow cytometry. These adNSCs can further differentiate into astrocytes, oligodendrocytes, and functional neurons, which were able to generate tetrodotoxin-sensitive sodium current. Additionally, we found that the neural differentiation of hAD-MSCs were significantly suppressed by *Sox1* interference, and what's more, Step1 was a key step for the following induction, probably because it was associated with the initiation and nuclear translocation of *Sox1*, an important transcriptional factor for neural development. Finally, we observed that bone morphogenetic protein signal was inhibited, and Wnt/β-catenin signal was activated during inducing process, and both signals were related with *Sox1* expression. In conclusion, we successfully established a three-step inducing protocol to derive NSCs from hAD-MSCs with high purity by *Sox1* activation. These findings might enable to acquire enough autologous transplantable NSCs for the therapy of neurodegenerative diseases in clinic.

Introduction

Nerve injury and neurodegenerative disorders characterized by loss or dysfunction of neural cells are major problems in clinic, and there are still no effective treatments [1–3]. The emerging of stem cell-based therapy provides a potential solution to this problem. Neural stem cell (NSC) is a kind of adult stem cell with multipotency and can differentiate into neural lineage cell, such as neuron, astrocyte, and oligodendrocyte [4]. In vivo transplantation of NSCs reduced neuronal damage and significantly improved the motor function of brain injury in mouse [5,6]. Recently, other reports declared that NSCs could promote regeneration through neuroprotection or immunomodulation. Intraventricular-transplanted NSCs could migrate to the inflamed area to downregulate the inflammatory brain process and to attenuate the severity of autoimmune encephalomyelitis [7–11]. Additionally, NSCs transplanted by intravenous injection also have similar functions. They transiently appeared in lymph nodes and spleen and inhibited the activation and proliferation of T cells, which could inhibit encephalomyelitis and reduce central nervous system (CNS) inflammation and tissue injury through immunosuppression [12,13]. Thus, NSC is considered an ideal candidate seed cell of stem cell-based treatment of neurodegenerative diseases [14]. NSCs can be isolated from fetal and adult CNS [15,16] or generated from embryonic stem cells (ESCs) and induced pluripotent stem cells [17,18]; however, it is hard to get enough transplantable NSCs for clinical treatment. Therefore, it is necessary to find other approach to get enough suitable seed cells.

Mesenchymal stem cell (MSC) is another adult stem cell first isolated from bone marrow [19] and has become an attractive cell source for regenerative medicine. Now, MSC can be obtained from various tissues, including adipose tissues,

[1]Center of Excellence in Tissue Engineering, Chinese Academy of Medical Sciences and Peking Union Medical College, Institute of Basic Medical Sciences and School of Basic Medicine, Beijing, People's Republic of China.
[2]Peking Union Medical College Hospital, Beijing, People's Republic of China.

which is easily obtained from patients by less invasive methods, such as lipoaspiration [20]. Adipose-derived MSCs (AD-MSCs) possess similar characteristics and differentiation potential with bone marrow MSCs (BMSCs) [21,22]. The advantages of large quantity and easily accessiblity make autologous AD-MSCs one of the most ideal cell sources and might be applied as substitute of BMSCs for the stem cell-based regenerative medicine [23,24]. Generation of NSCs from AD-MSCs will provide a large number of cell sources for the treatment of neurodegenerative disorders.

Some reports have demonstrated the possibility of neural differentiation potential of human AD-MSCs (hAD-MSCs). However, most cells they got were fully differentiated neural cells and possess limited regenesis capacity. The differentiation of hAD-MSCs into NSCs was rarely reported. Hsueh et al. observed that, when seeded on a chitosan-coated surface, hAD-MSCs can form spheres containing 19.5% ± 2.6% *Nestin*-positive cells [25]. Ahmadi et al. also reported that, after cultured in the serum-free medium, 51% ± 13.22% *Nestin*-positive cells could be generated from hAD-MSCs [26]. However, there were no functional detections especially the electrophysiology analysis in both researches. So, whether these *Nestin*-positive cells they finally got can differentiate into functional sublineages remains unknown. Moreover, the *Nestin*-positive cells were mixed with *Nestin*-negative nonneural cells, which is unsuitable for clinic application.

Embryogenesis is regulated by the sequentially activation and inactivation of transcriptional factors. So, it is a good way to induce cell differentiation by mimicing the sequentially changes of specific transcriptional factors or markers. In the process of human neural development, the initiation of neuroectoderm begins with *Pax6* expression, followed by *Sox1*, which subsequently regulates the expression of downstream genes, such as *Nestin* [27–29]. *Pax6* and *Sox1* are important factors in the development of early nerve central system and considered markers of early NSCs.

In this study, we found that there was a moderate expression of *Pax6* in hAD-MSCs. So, we established a three-step protocol to generate NSCs from hAD-MSCs by activating *Sox1* expression. Early NSCs markers *Sox1, Pax6* as well as *Nestin* and *Vimentin* were used for the characterization of hAD-MSC-derived NSCs (adNSCs). Then, the differentiation ability to neurons, astrocytes, and oligodendrocytes of adNSCs was tested in the terminal differentiation medium; electrophysiology analysis for functional neurons and enzyme-linked immunosorbent assay analysis detection for neutrophic factors in culture supernatant of glia cells were used for the functional analysis of terminal differentiated cells from adNSCs. Finally, the mechanism was investigated. To the best of our knowledge, we are the first to generate functional NSCs from hAD-MSCs with high purity by activating transcriptional factor for early neural development.

Materials and Methods

Isolation of hAD-MSCs and neural differentiation

Adipose tissue was obtained from human liposuction aspirates with informed consent of the donors (25–35 years old) and was performed according to the procedure provided by the Ethics Committee at the Chinese Academy of Medical Sciences and Peking Union Medical College. Isolation of AD-MSCs was performed as previous report [30]. hAD-MSCs were resuspended in the culture medium and seeded at a density of 2×10^6 cells per dish (10 cm). Cultures were maintained in a 37°C incubator with 5% CO_2 and passaged with trypsin/ethylenediaminetetraacetic acid when cells were confluent. hAD-MSCs isolated from 10 different donors (six females and four males) were used in our study.

To initiate differentiation into NSCs, hAD-MSCs at passage 3 were used (Fig. 1). At first (Step1), $Sox1^{low}/Nestin^{low}$ hAD-MSCs were seeded on gelatin-coated 10-cm dishes at a density of 2×10^6 and pre-induced in the pre-inducing medium (knockout Dulbecco's modified Eagle's medium (DMEM) supplement with 20% serum replacement, 1 mM L-glutamin, 1% nonessential amino acid, 0.1 mM β-mercaptoethanol, 4 ng/mL basic fibroblast growth factor (bFGF) for 8 days to activate Sox1 expression. Then (Step2), $Sox1^{moderate}/Nestin^{low}$ cells were cultured in the N2B27 medium consisting of the Neural basal medium: DMEM/F12 (1:1) supplemented with 1 mM L-glutamin, 2% B27, 1% N2, and 0.1 mM β-mercaptoethanol. Seven days later, *Sox1* expression was increased and the medium was replaced by the N2B27 medium supplement with 20 ng/mL epidermal growth factor (EGF), 20 ng/mL bFGF for another 7 days to generate adNSCs (Step3). A human neuroblastoma cell line SH-Sy5y was used as a positive control.

Terminal differentiation ability of adNSCs was tested according to previous report [31]. Briefly, cells were seeded on poly-D-lysine and laminin-coated plastic coverslips (Nunc) and cultured in the Neurobasal medium supplemented with 1% N2 supplement, 1% fetal calf serum, 5% horse serum, and 0.5 mM all-trans-retinoic acid for 2 weeks. 10 ng/mL of platelet-derived growth factor (PDGF)-BB and brain-derived neurotrophic factor (BDNF) were added for glial induction and neuronal induction, respectively. Two weeks later, cells were prepared for detection.

Transfection of small-interfering RNAs

Small-interfering RNAs (siRNAs) of *Sox1* (siSox1) were used to suppress *Sox1* expression. siSox1 (UGAAGGAG

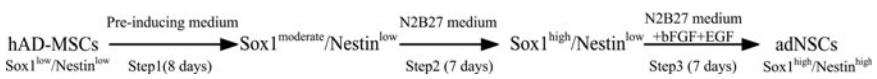

FIG. 1. Differentiation procedure from human adipose-derived mesenchymal stem cells (hAD-MSCs) to neural stem cells (NSCs) (hAD-MSC-derived NSCs, adNSCs). hAD-MSCs ($Sox1^{low}/Nestin^{low}$) were cultured in the pre-inducing medium for 8 days to activate *Sox1* expression. Then, $Sox1^{moderate}/Nestin^{low}$ cells were cultured in the N2B27 medium for 7 days to promote *Sox1* expression. Finally, the medium was changed to the N2B27 medium containing basic fibroblast growth factor (bFGF) and epidermal growth factor (EGF), and cells were cultured for another 7 days to generate $Sox1^{high}/Nestin^{high}$ adNSCs.

CACCCGGAUUATT) and negative control (siNC) (UUC UCCGAACGUGU CACGUTT) were purchased from Invitrogen. siRNAs were transfected into cells at Step1 with lipofectamine 2000 (Invitrogen) according to the manufacturer's instruction. mRNA and protein samples were collected at 24 or 48 h after transfection to detect the efficiency of interference.

RNA isolation and quantitative reverse transcription–polymerase chain reaction

Total RNA was extracted using TRIzol reagent (Invitrogen) and treated with DNase I (Promega). First-strand cDNA was synthesized with 2 μg total RNA in 30 μL using a revertAid™ first-strand cDNAs ynthesis kit (Fermentas) according to the manufacturer's instruction. Quantitative polymerase chain reaction (qPCR) analyses were performed in triplicate using SYBR Green master mixture, and gene expression data were detected using ABI stepone plus 7500 system. The thermal parameters were 95°C for 1 min, followed by 40 cycles of 95°C for 10 s and 60°C for 40 s. Gene expression level was normalized by *GAPDH* housekeeping gene expression. The primer sequences used in our study were listed in Table 1.

Preparation of frozen sections

hAD-MSC-derived neurospheres were collected by centrifugation at 800 rpm for 3 min and fixed with 4% paraformaldehyde (PFA) for 30 min at room temperature. Then, PFA were removed and washed in PBS for three times; spheres were transferred sequentially to 10%, 20%, and 30% sucrose solution for 30 min, respectively, and water inside spheres was dehydrated. After that, spheres were placed in a small container with smooth bottom and gathered using a syringe needle. Then, spheres were embedded with optical cutting temperature compound and frozen immediately at −80°C. Frozen spheres were dissected to 6 μm each and placed on adhesion microscope slides. Frozen sections can be stored at −80°C for long storage.

Immunofluorescence staining

Samples were fixed at room temperature with 4% PFA for 10 min (this step can be omitted for frozen sections). After premeablization in 1% triton X-100/PBS for 15 min, nonspecific binding were blocked with 3% bovine serum albumin for 1 h at 37°C. Then, samples were incubated in primary antibodies at the appropriate dilution at 4°C

Table 1. Primers Used in this Study

Gene	*Sense primer (5′–3′)*	*Antisense primer (5′–3′)*
Sox1	CCTCCGTCCATCCTCTG	AAAGCATCAAACAACCTCAAG
Pax6	AGGTATTACGAGACTGGCTCC	TCCCGCTTATACTGGGCTATTT
Nestin	CAACAGCGACGGAGGTCTC	CCTCTACGCTCTCTTCTTTGAGT
Vimentin	AGAACTTTGCCGTTGAAGCTG	CCAGAGGGAGTGAATCCAGATTA
Sox2	AGTCTCCAAGCGACGAAAAA	GCAAGAAGCCTCTCCTTGAA
Sox3	GACCTGTTCGAGAGAACTCATCA	CGGGAAGGGTAGGCTTATCAA
Musashi-1	TTCGGGTTTGTCACGTTTGAG	GGCCTGTATAACTCCGGCTG
Olig2	GCTGCGACGACTATCTTCCC	GCCTCCTAGCTTGTCCCCA
FoxG1	AGAAGAACGGCAAGTACGAGA	TGTTGAGGGACAGATTGTGGC
Gli3	TGGTTACATGGAGCCCCACTA	GAATCGGAGATGGATCGTAATGG
Emx1	AAGCGCGGCTTTACCATAGAG	GCTGGGGTGAGGGTAGTTG
Emx2	CGGCACTCAGCTACGCTAAC	CAAGTCCGGGTTGGAGTAGAC
Nkx2.1	AGCACACGACTCCGTTCTC	GCCCACTTTCTTGTAGCTTTCC
Gsh2	ATGTCGCGCTCCTTCTATGTC	CAAGCGGGATGAAGAAATCCG
Otx2	CCCCACTGTCAGATCCCTTG	TGAAGCCTGAGTATAGGTCATGG
Six3	CAAGGAGTCTCACGGCAAG	GCAATGCGTCTTCTGCTCG
SCN5A	CCTAATCATCTTCCGCATCC	TGTTCATCTCTCTGTCCTCATC
NE-NA	GCTCCGAGTCTTCAAGTTGG	GGTTGTTTGCATCAGGGTCT
Maxik	ACAACATCTCCCCCAACC	TCATCACCTTCTTTCCAATTC
KV1.4	ACGAGGGCTTTGTGAGAGAA	CACGATGAAGAAGGGGTCAT
KV4.2	ACCGTGACCCAGACATCTTC	CACTGTTTCCACCACATTCG
KV4.3	GCCTCCGAACTAGGCTTTCT	CCCTGCGTTTATCAGCTCTC
EAG1	TGGATTTTGCAAGCTGTCTG	GAGTCTTTGGTGCCTCTTGC
EAG2	ACATCCTGCTTTTCGATTGG	CGGCTCTCTACCTGGCGTTG
CACNA1C	AACATCAACAACGCCAACAA	AGGGCAGGACTGTCTTCTGA
CACNA1G	CTGCCACTTAGAGCCAGTCC	TCTGAGTCAGGCATTTCACG
BDNF	CTACGAGACCAAGTGCAATCC	AATCGCCAGCCAATTCTCTTT
NT3	CATTCGGGGACACCAGGTC	TTTGCACTGAGAGTTCCAGTGTTT
NT4	CAAGGCTGATAACGCTGAGGAAGG	GGTCAATGCCCGCACATAGGA
GDNF	GGCAGTGCTTCCTAGAAGAGA	AAGACACAACCCCGGTTTTTG
NGF	GGCAGACCCGCAACATTACT	CACCACCGACCTCGAAGTC
CyclinD1	GCTGCGAAGTGGAAACCATC	CCTCCTTCTGCACACATTTGAA
c-Myc	GGCTCCTGGCAAAAGGTCA	CTGCGTAGTTGTGCTGATGT
BMP2	ACCCGCTGTCTTCTAGCGT	TTTCAGGCCGAACATGCTGAG
BMP4	AAAGTCGCCGAGATTCAGGG	GACGGCACTCTTGCTAGGC
GAPDH	GGTCACCAGGGCTGCTTTTA	GAGGGATCTCGCTCCTGGA

overnight. Secondary antibodies were used for 1 h at 37°C after washing with PBS. Hochest courterstain were used for visualization. Pictures were captured using Olympus inverted fluorescence microscope. The following antibodies were used: *Sox1* (rabbit IgG, 1:100, ab109290; Abcam), *Pax6* (rabbit IgG, 1:100, ab5790; Abcam), *Nestin* (mouse IgG, 1:200, ab22035; Abcam), *Vimentin* (mouse IgG, 1:50, sc6260; Santa Cruz), *MAP2* (mouse IgG, 1:200, ab11267; Abcam), *GFAP* (goat IgG, 1:200, ab53554; Abcam), *O4* (mouse IgM, 1:100, MAB345; Millipore), goat anti-rabbit IgG –fluorescein isothiocyanate (FITC) (1:100, ZF0311; Zhong Shan Golden Bridge), goat anti-mouse IgG FITC (1:100, sc2010; Santa Cruz), goat anti-mouse IgM FITC (1:100, sc2082; Santa Cruz), and rabbit anti-goat FITC (1:100, ZF0314; Zhong Shan Golden Bridge).

Western blotting analysis

Protein lysates were prepared for western blot analysis using RIPA lysis buffer containing 1 mM phenylmethanesulfonyl fluoride and complete protease inhibitor; supernatant was collected by high-speed centrifuge (13,000 *g*, 4°C for 30 min). Protein concentration was detected using bicinchoninic acid kit according to the manufacturer's instruction. Then, total cell lysates containing equal amount of protein were separated on a 10% sodium dodecyl sulfate polyacrylamide gel electrophoresis gel and transferred to polyvinylidene fluoride membranes. The membranes were blocked in 5% nonfat milk for 1 h and incubated in primary antibodies overnight at 4°C, followed by corresponding horseradish peroxidase-conjugated secondary antibodies for 1 h at room temperature. Signals were visualized with an immobilon Western chemiluminescent HRP substrate (WBKLS0100; Millipore) and detected using ImageQuant LAS 4000mini imaging system. *β-actin* was used as an internal control. In some instances, the membranes were stripped and incubated with different antibodies. Primary antibodies used were as follows: *Sox1* (rabbit IgG, 1:1,000, ab109290; Abcam), *Pax6* (rabbit IgG, 1:1,000, ab5790; Abcam), *Nestin* (mouse IgG, 1:1,000, ab22035; Abcam), *Vimentin* (mouse IgG, 1:200, sc-6260; Santa Cruz), *β-catenin* (goat IgG, 1:200; Santa Cruz), *Smad1* (rabbit IgG, 1:1,000, 9743; Cell Signal), *p-Smad1* (rabbit IgG, 1:1,000, 9511; Cell Signal), and *β-actin* (mouse IgG, 1:5,000, sc47778; Santa Cruz); and HRP-conjugated anti-rabbit (sc-2004, 1:2,000; Santa Cruz), anti-goat (sc-2020, 1:3,000; Santa Cruz), or anti-mouse (sc-2005, 1:2,000; Santa Cruz) secondary antibodies were applied. Optical density of every band was detected by using Image J software. Relative protein expression was presented as normalized to β-actin.

Flow cytometry assay

hAD-MSC-derived neurospheres were dissociated into single cells by incubated in the accutase solution (Sigma) for 5 min at 37°C. After permeabilizated for 15 min at 4°C, cells were incubated with *Sox1* (rabbit IgG, ab109290; Abcam), *Pax6* (rabbit IgG, ab5790; Abcam), *Nestin* (mouse IgG, ab22035; Abcam), and *Vimentin* (mouse IgG, sc-6260; Santa Cruz) for 30 min on ice followed by three times wash. Then, the samples were incubated in secondary antibodies conjugated with FITC for another 30 min on ice. After washing, cells were fixed and fluorescence intensity was detected using BD Accuri C6 flow cytometer.

Electrophysiological detection

Plastic coverslips (Nunc) containing a monolayer cells were transferred to a recording chamber on the stage of an inverted microscope. The culture medium was replaced with extracellular solution containing: 140 mM NaCl, 5 mM KCl, 1 mM $CaCl_2$, 1 mM $MgCl_2$, 10 mM glucose, 10 mM HEPES (pH = 7.3); pipettes were filled with an intracellular-like solution containing 140 mM KCl, 5 mM NaCl, 1 mM $CaCl_2$, 10 mM HEPES, 5 mM EGTA, 2 mM Mg-ATP according to previous report [32]. The resistant of fire-polished pipettes was 5–10 MΩ. All experiments were performed at room temperature. Tetrodotoxin (TTX) was added to the extracellular solution to block the sodium current. Ionic currents were recorded using the patch-clamp whole-cell configuration with an axoclamp 700B patch-clamp amplifier and digitized using a digidata 1322A A/D converter. Data were analyzed using pClamp10.1 and Originpro 8.0 software.

Enzyme-linked immunosorbent assay analysis

To detect the secretion of neurotrophic factors in adNSC-derived glia cells, the culture medium was replaced 24 h before collection; the secretion of *BDNF*, neurotrophin 3 (*NT3*), neurotrophin 4 (*NT4*), glial cell line derived neurothropic factor (*GDNF*) and nerve growth factor (*NGF*) were assayed by enzyme-linked immunosorbent assay kits according to the manufacturer's instructions (Senxiong Biotech).

Statistical analysis

Each experiment was performed at least three times; data were presented as mean ± SD. Statistical significance was tested by two-tailed Student's *t*-test or ANOVA using SPSS statistics 13.0. A value of $P < 0.05$ was considered statistically significant (indicated by "*").

Results

Generation of adNSCs from hAD-MSCs by a three-step induction

hAD-MSCs were maintained as subconfluent cultures and grew in a monolayer with typical fibroblast-like morphology (Fig. 2A-a). After cultured in the pre-inducing medium (Step1), cells showed a significant morphological change from fibroblast-like cells to flat morphology with obscure boundary (Fig. 2A-b). Eight days later, the pre-inducing medium was replaced by the N2B27 medium, which was commonly used in neural induction process from ESCs. Then, 7 days later, flat cells began to retract and become smaller and showed uniform morphology (Fig. 2A-c). After that, the medium were replaced by N2B27 supplemented with bFGF and EGF. After 7 days of culture, cells exhibit distinct biopolar or multipolar morphologies with branched processes (Fig. 2A-d), which is similar to monolayer NSCs reported by Sun et al. [16]. They could easily be detached from the bottom after digestion and gathered together to form neurospheres when cultured in ultra-low dishes (Fig. 2B). Passage was performed mechanically every week for three to five times.

Identification of adNSCs

Immunofluorescence detection showed that undifferentiated hAD-MSCs expressed moderate level of *Pax6* and

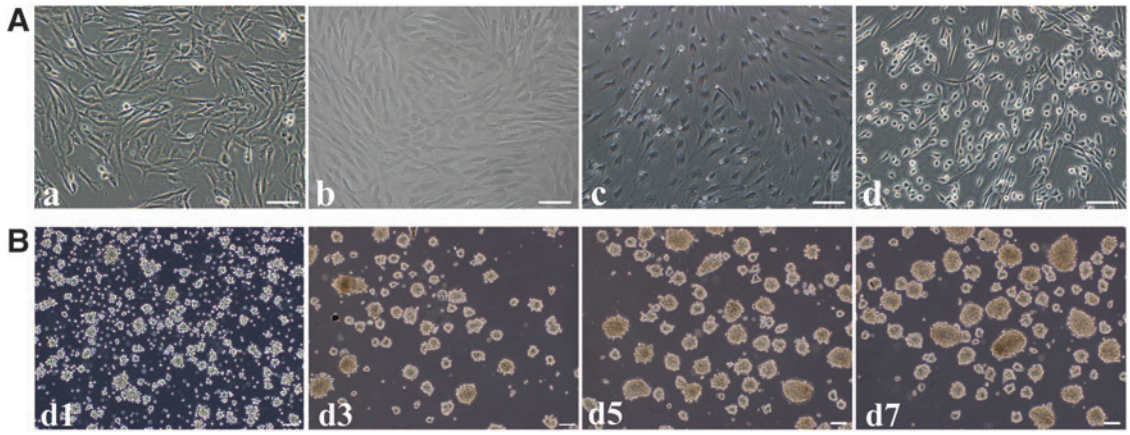

FIG. 2. Differentiation of hAD-MSCs into adNSCs. **(A)** Cell morphology of hAD-MSCs **(a)**, after pre-induction (Step1) **(b)**, cultured in the N2B27 medium (Step2) for 7 days **(c)**, and cultured in the N2B27 medium containing bFGF and EGF (Step3) (adNSCs) for another 7 days **(d)**. **(B)** Expansion of neurospheres. Spheres cultured in suspension at d1, d3, d5, d7 after passage. Bar = 100 μm.

Vimentin, and no expression of *Sox1* and *Nestin*. After induction, adNSCs cultured as monolayer or neurospheres highly expressed *Sox1, Pax6, Nestin*, and *Vimentin* (Fig. 3A); however, the expression of *Pax6* (transcriptional factor) was detected in the cytoplasm of both undifferentiated hAD-MSCs and adNSCs, whereas *Sox1* (transcriptional factor) expressed in the nucleus of adNSCs. The increasing expression of NSCs markers were also verified by western blot analysis (Fig. 3B and Supplementary Fig. S1; Supplementary Data are available online at www.liebertpub.com/scd). While the difference was that, there was low expression of *Sox1* and *Nestin* in hAD-MSCs. After pre-inducing step (Step1), *Sox1, Nestin, Pax6*, and *Vimentin* were increased. We also found that there existed similar expression pattern of *Sox1* and *Nestin*; it was consistent with the gene expression pattern during early neuroectoderm development, which also means that the differentiation process may be in line with the developmental sequence in vivo. Furthermore, we observed that adNSCs had similar expression level of *Sox1* with SH-Sy5y (positive control). The mRNA expression levels of genes associated with embryonic neural development and neural differentiation, such as *Sox1, Pax6, Nestin, Vimentin, Sox2, Sox3,* Musashi-1, *Olig2, Gli3, Emx1, Emx2, Gsh2, Nkx2.1, FoxG1, Otx2*, and *Six3*, were increased compared to hAD-MSCs ($^*P < 0.05$) (Fig. 3C). Furthermore, the proportion of *Sox1*-, *Pax6*-, *Nestin*-, and *Vimentin*-positive cells in neurospheres was 96.1% ± 1.3%, 96.8% ± 1.7%, 96.2% ± 1.3%, and 97.2% ± 2.5%, respectively, by flow cytometry analysis (Supplementary Fig. S2).

adNSCs can differentiate into functional neurons, astrocytes, and oligodendrocytes

To detect the terminal differentiation ability of adNSCs, adNSCs were cultured in the terminal differentiation medium with *BDNF or PDGF*. After 2 weeks of induction, cells cultured in the neuron induction medium showed neural-like structure with small cell body and long processes, they connected with each other and formed net structures (Fig. 4A-a, b). These neuron-like cells expressed *MAP2*, a marker expressed on mature neurons (Fig. 4A-c). To assess whether these neuron-like cells possess function, inward sodium current, which is responsible for the production of action potentials in neural cells, was detected using the patch clamp technique in whole-cell recording model. Undifferentiated hAD-MSCs were quiescent, and no inward sodium current was detected (Fig. 4B-a). On the contrary, neuron-like cells displayed a voltage-dependent sodium current, which showed a feature of fast activation and fast inactivation. The mean peak amplitude at −10 mV was −438 ± 20 pA (Fig. 4B-b, d). These sodium currents could be blocked by 500 nM TTX (Fig. 4B-c), a sodium channel blocker. Besides functional study, we also examined the mRNA expression of ion channel genes using qPCR (Fig. 4C). We found that the expression of sodium ion channel genes *SN5A, NE-NA*, potassium ion channel genes *MaxiK, KV4.3, KV4.2, KV1.4, EAG1, EAG1*, and calcium ion channel genes *CACNA1C, CACNA1G* all increased compared to undifferentiated hAD-MSCs ($^*P < 0.05$). Moreover, $GFAP^+$ and $O4^+$ cells were also observed in the glial induction medium, which exhibited astrocyte- or oligodendrocyte-like shape (Fig. 4D). The mRNA expression of neurotrophic-associated genes, *BDNF, NT3, NT4, GDNF*, and *NGF*, significantly increased in these cells compared to hAD-MSCs ($^*P < 0.05$) (Fig. 4E); the secretion of *BDNF, NT3, NT4, GDNF*, and *NGF* in 24 h (10^5cells) in supernatant was 180 ± 13.5 pg/mL, 1050 ± 23.5 pg/mL, 1700 ± 34.6 pg/mL, 217.7 ± 15.9 pg/mL, and 900 ± 18.4 pg/mL, respectively (Fig. 4F), which implied their neurotrophic factor-secretion function.

Differentiation of hAD-MSCs to NSCs was inhibited by Sox1 *interference*

During embryogenesis process, *Sox1* is an important transcriptional factor in early neural development and is considered an early marker of NSCs. To investigate the functional effect of *Sox1* on NSCs differentiation of hAD-MSCs, *Sox1* activation at Step1 was suppressed by transfecting siRNA of *Sox1* (siSox1). As shown in Fig. 5A and B, after transfection, both mRNA and protein expression of *Sox1* was downregulated at the end of Step1. The cells transfected with siSox1 or siNC were then induced to

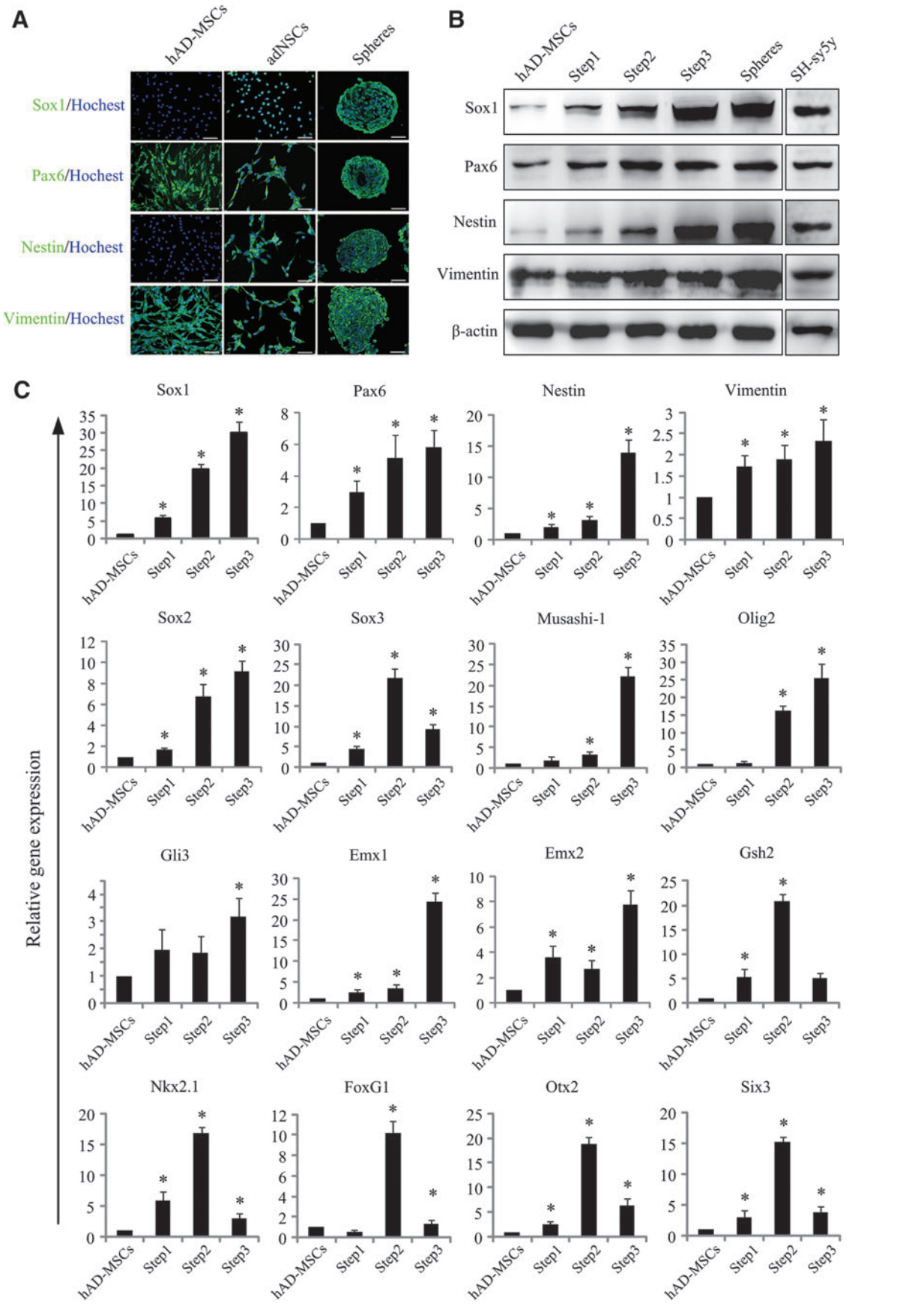

FIG. 3. Identification of adNSCs. **(A)** Immunostaining of NSCs markers *Sox1*, *Pax6*, *Nestin*, and *Vimentin* in undifferentiated hAD-MSCs, adNSCs culture monolayer and neurospheres. adNSCs we obtained expressed NSCs markers both in monolayer and in neurospheres. Bar = 100 μm. **(B)** Western blot analysis. **(C)** Expression of genes associated with embryonic neural development during induction (*$P < 0.05$ compared with hAD-MSCs).

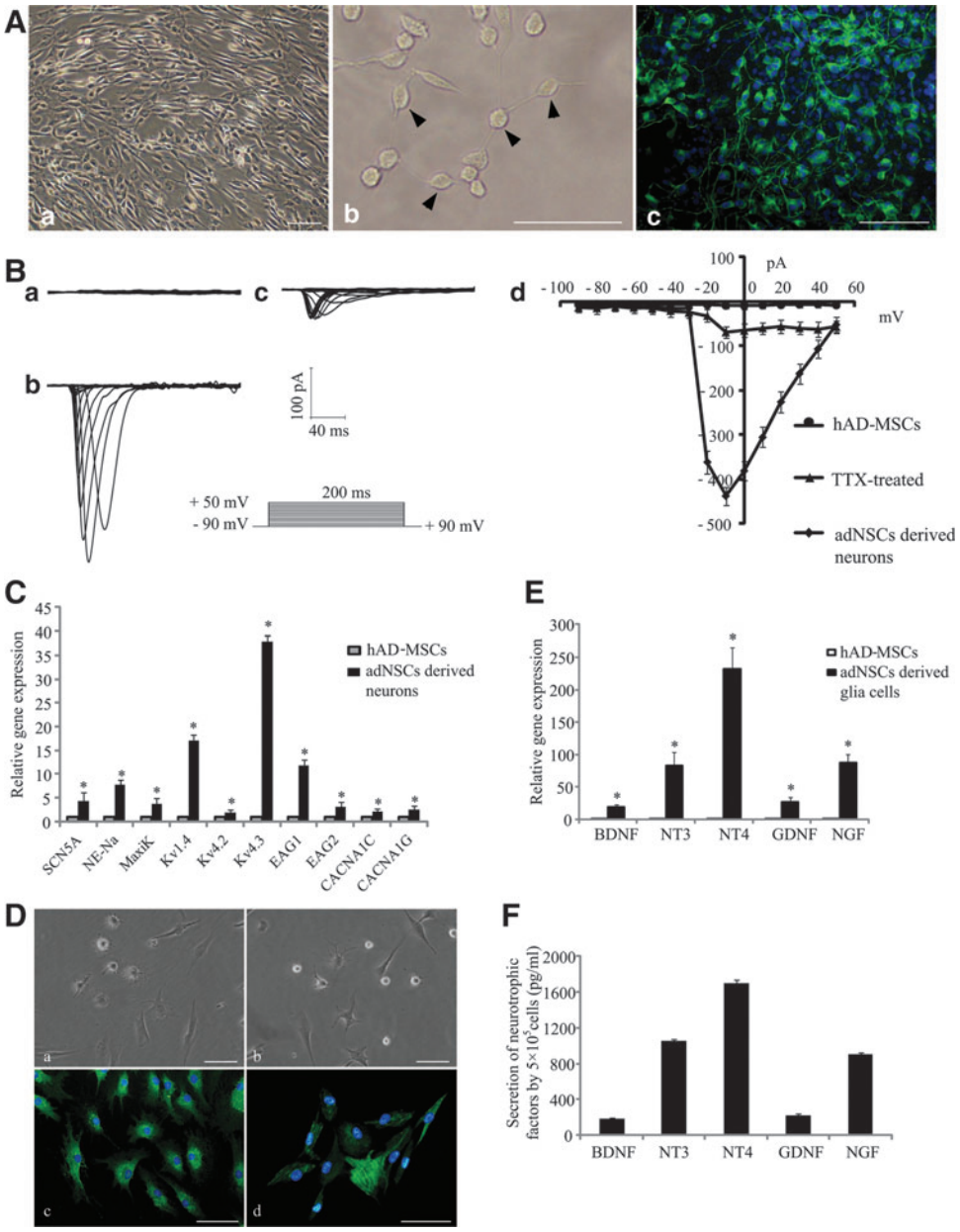

FIG. 4. Terminal differentiation of adNSCs. **(A)** adNSC-derived neurons **(a, b)** and characterization of neurons by immunostaining for mature neurons marker MAP2 (*green*) **(c)**. Bar = 100 μm. **(B)** Electrophysiological analysis for inward sodium current. No inward sodium current was detected in hAD-MSCs **(a)**. Voltage-dependent sodium current was detected in adNSC-derived neurons **(b)**, this current can be blocked by 500 nM tetrodotoxin (TTX) **(c)**. The peak current–voltage relationship was plotted against the voltages **(d)**. **(C)** Gene expression of ion channel markers. Gene expression of ion channel markers increased significantly compared with hAD-MSCs (*$P < 0.05$). **(D)** Glia differentiation of adNSCs. adNSCs can differentiate into astrocytes **(a)** and oligodendrocytes **(b)**. *GFAP* expression (*green*) in astrocytes **(c)** and *O4* expression (*green*) in oligodendrocytes **(d)** by immnostaining. Bar = 100 μm. **(E)** Examination of gene expression of neurotrophic factors in adNSC-derived glia cells. Gene expression of neurotrophic factors significantly increased compared with hAD-MSCs (*$P < 0.05$). **(F)** Secretion of neurotrophic factors in 24 h in the culture surpernanant of adNSC-derived glia cells by enzyme-linked immunosorbent assay analysis. All data represent mean ± standard deviation, $n = 3$.

differentiate into NSCs. Real-time PCR and western blot analysis showed that, compared with siNC group, the mRNA and protein expression of NSCs markers in adNSCs were significantly repressed in siSox1 group as a result of *Sox1* suppression (*$P < 0.05$) (Fig. 5C, D). Consistent with these results, flow cytometry analysis demonstrated that the percentage of *Sox1*- and *Nestin*-positive cells in siSox1 group was much lower than siNC group (Supplementary Fig. S3). All these results indicated that *Sox1* played an important in role in the differentiation of hAD-MSCs into NSCs.

Pre-inducing step (step 1) was essential for the expression and nuclear translocation of Sox1

In our study, the results showed that *Sox1* played key role during the induction process, and we observed that *Sox1* was activated after pre-inducing process. So, we questioned that what does the pre-inducing step function for the whole induction process. To investigate this question, hAD-MSCs were divided into two groups: pre-inducing step containing group (pre^+ group) and pre-inducing step omitted group (pre^- group). Cells in pre^+ group were induced in the induction system we established above, whereas cells in pre^- group were cultured in the N2B27 medium followed by the N2B27 medium supplement with bFGF and EGF, in which pre-inducing step was omitted. The expression of NSC markers in hAD-MSCs and cells finally obtained in both groups were detected by qPCR and western blot analysis. In pre^- group, cells remained a fibroblast-like shape after induction, a bit different from hAD-MSCs (Fig. 6A). There existed *Sox1*- and *Nestin*-positive cells in pre^- group by immunofluorescence staining; however, the expression were very low (Fig. 6B). On the contrary, the expression of *Sox1*, *Pax6*, *Nestin*, and *Vimentin* in adNSCs with pre-inducing step

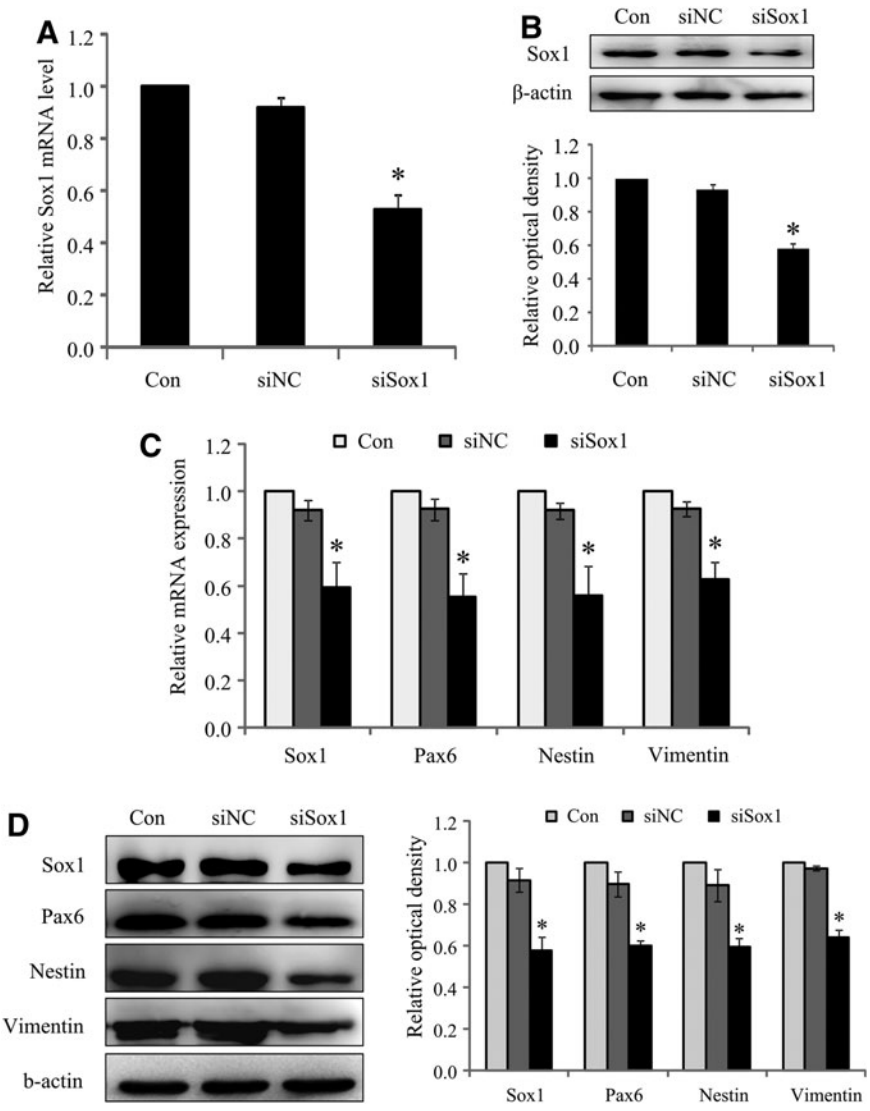

FIG. 5. *Sox1* inhibition suppresses the differentiation of hAD-MSCs into NSCs. **(A)** Real-time PCR analysis of the *Sox1* mRNA level after transfection with small-interfering RNAs (siSox1 or siNC). **(B)** Protein level of *Sox1* after transfection with siSox1 or siNC by western blot analysis, relative optical density was measured. **(C)** mRNA expression of NSC markers of adNSCs after *Sox1* or NC transfection. **(D)** Protein level of NSCs markers after transfection with siSox1 or siNC by western blot analysis, relative optical density was measured. (All data displayed as mean ± standard deviation, $n = 3$.*$P < 0.05$ compared with the siNC group).

(pre$^+$ group) were significant higher than pre$^-$ cells both in protein and mRNA levels (*$P < 0.05$) (Fig. 6C, D). This indicated that the pre-inducing step played an important role in the activation of *Sox1* and was essential for the following induction.

To investigate the relationship between pre-inducing process and *Sox1* activation, hAD-MSCs were cultured in the pre-inducing medium for 8 days, samples were collected every 2 days, qPCR and immunofluorescence staining was used to detect *Sox1* expression. There was an obviously cell morphological change from fibroblast-like cells at day 0 to flat shape at day 8, this was identical with the results above (Fig. 7A phase-contrast). The mRNA and protein expression of *Sox1* gradually increased as time extended and achieved to a peak at day 8 (Fig. 7B, C). Furthermore, there was an obvious nuclear translocation of *Sox1* in this process (Fig. 7D). After 2 days of induction (d2), *Sox1* was initiated and expressed in cytoplasm and perinuclear area. Two days later (d4), fluorescence signals began to appear both in cytoplasm and in nucleus. Then, *Sox1* protein expressed in cytoplasm was gradually transferred to nucleus. This translocation process was completed at day 8, and *Sox1* mainly accumulated to the nucleus. All results indicated that the pre-inducing culture environment could promote the activation and nuclear translocation of *Sox1*, where it functioned as a transcriptional factor.

Signals involved in the generation of adNSCs from hAD-MSCs

Pre-inducing medium is a serum-free mixture. It contains only one cytokine-bFGF, which was reported to play important roles in neural differentiation [33]. To find out whether it functioned in *Sox1* expression, the relationship of bFGF with *Sox1* expression was detected. hAD-MSCs were cultured in the pre-inducing medium containing 0, 4, 10, 20, 50, and 100 ng/mL bFGF, respectively, for 8 days. mRNA samples were collected every other day. The expression of *Sox1* was detected by qPCR. The expression of *Sox1* increased in every group cultured in the medium supplemented with different concentrations of bFGF as time extended. However, there was no obvious difference of *Sox1* expression at the same time point between the groups cultured with different concentration of bFGF (Fig. 8).

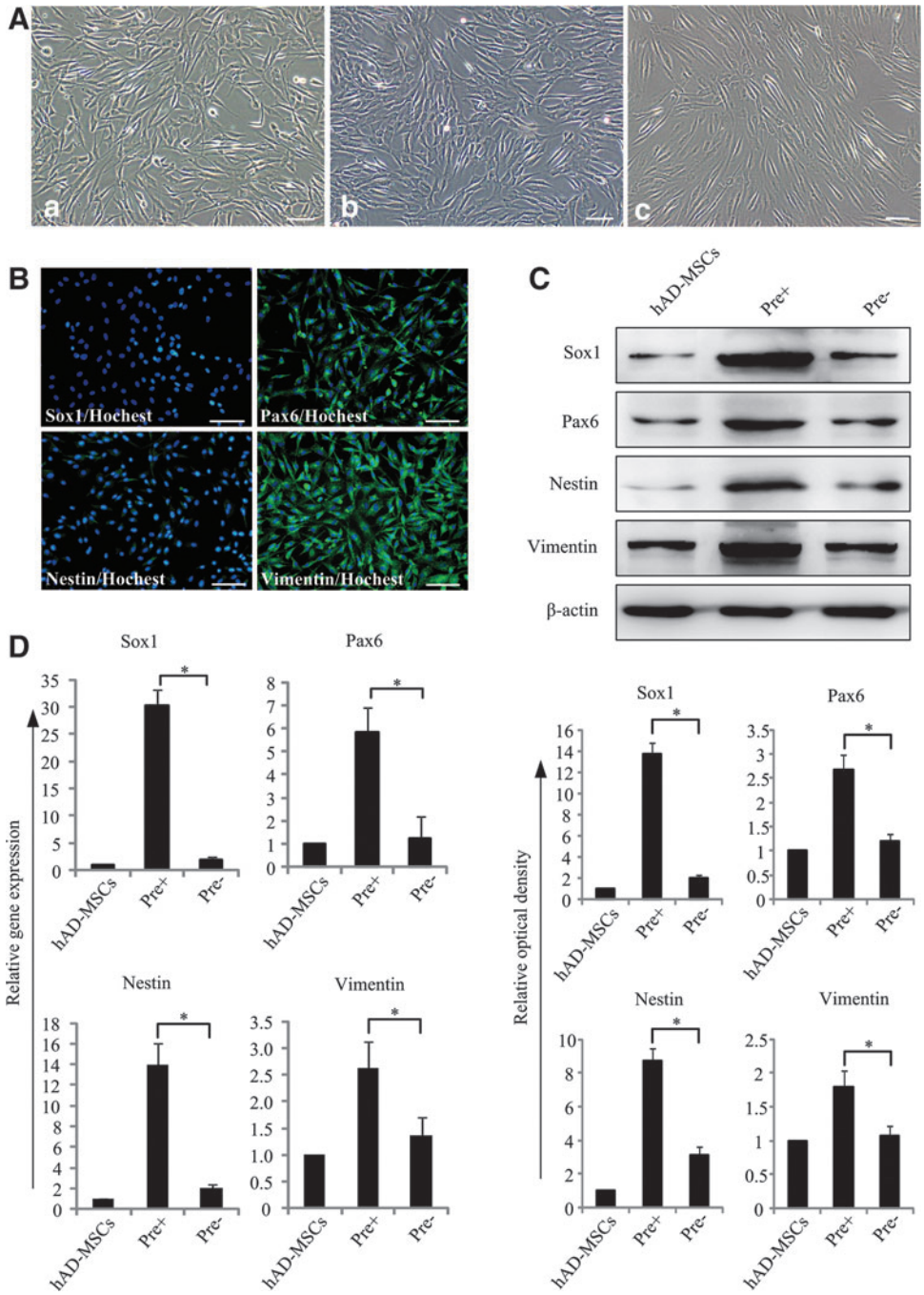

FIG. 6. **(A)** Cell morphology in the pre$^-$ group for which pre-inducing step was omitted. hAD-MSCs **(a)**, cells cultured in N2B27 for 7 days **(b)**, then cultured in the N2B27 medium containing bFGF and EGF for 7 days **(c)**. Bar = 100 μm. **(B)** Immunostaining for NSCs markers in cells of pre$^-$ group. Western blot **(C)** and qPCR analysis **(D)** of NSCs markers in cells finally obtained in the pre$^+$ group and pre$^-$ group. These results showed that when pre-inducing step was omitted (pre$^-$ group), the expression of NSCs markers greatly decreased in both mRNA and protein levels compared to the pre$^+$ group (*$P < 0.05$).

To determine whether signals functioned in early neural development were also involved in the generation of adNSCs, we examined the activation state of *Wnt/β-catenin* and bone morphogenetic protein (BMP) signal pathway. Our results showed that the expression of genes downstream of *Wnt/β-catenin* pathway such as *CyclinD1* and c-Myc increased, although mRNA expression of *BMP2* and *BMP4* (two ligands of *BMP* signal) decreased (Fig. 9A). These results were also confirmed by western blot analysis (Fig. 9B). We found that there existed very low expression of *β-catenin* (a signal effector in *Wnt/β-catenin* pathway) in undifferentiated hAD-MSCs; after cultured with the pre-inducing medium, *β-catenin* significantly increased (*$P < 0.05$ vs. hAD-MSCs) and maintained at the same level in the following steps, indicating that *Wnt/β-catenin* pathway was activated. As to *BMP* signal, although the expression of *Smad1* had no change, its activated form phosphorylated Smad1 (*p-Smad1*) were highly expressed in hAD-MSCs, then, *p-Smad1* began to decrease at Step1 (pre-inducing step), and nearly disappeared in Steps 2 and 3, which meant that *BMP* pathway was inhibited in this process. However, no difference was observed for the activation state of *Wnt/β-catenin* and *BMP* signals in pre$^-$ group for which pre-inducing step (Step1) was omitted (Fig. 9C).

To find out the relationship between *Sox1* and *Wnt/β-catenin* as well as *BMP* signals, hAD-MSCs were cultured in the pre-inducing medium contained BMP4 (10 ng/mL) or DKK1 (100 ng/mL), which activate *BMP* signal or inhibit the activation of *Wnt/β-catenin*, respectively. The expression of

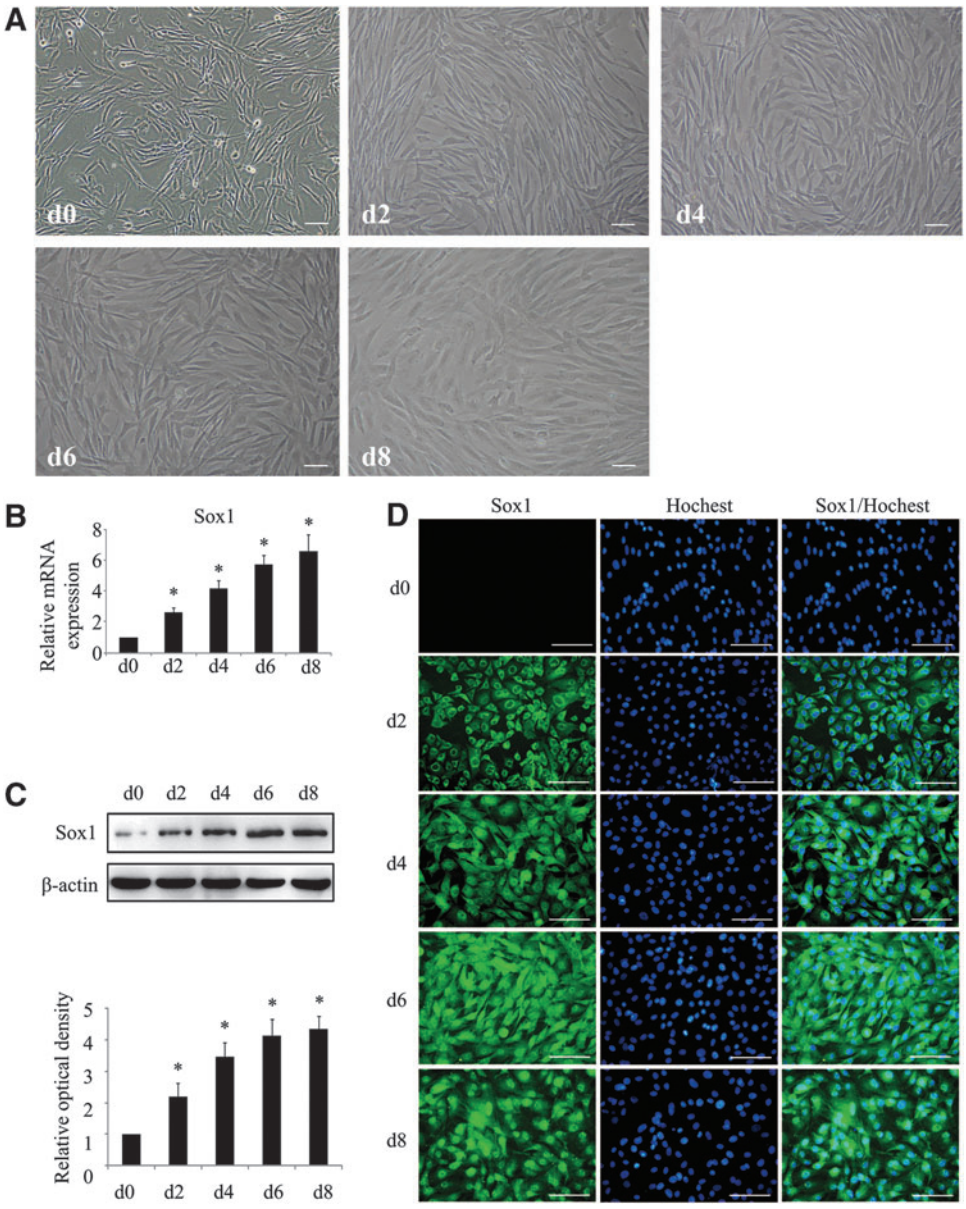

FIG. 7. Nuclear translocation of *Sox1* during pre-inducing process. **(A)** Cell morphorlogy at d0, d2, d4, d6, and d8 after cultured in the pre-inducing medium. Real-time PCR **(B)**, western blot analysis **(C),** and immunostaining **(D)** of *Sox1* expression. Bar = 100 μm. All data represent mean ± standard deviation, $n = 3$ (*$P <$ 0.05 compared with d0).

Sox1 was detected by western blot. We found that the addition of BMP4 or DKK1 increased the expression of *p-Smad1* or decreased the accumulation of β-catenin, and *Sox1* expression was decreased in both conditions compared with the BMP4$^-$ or DKK1$^-$ group (*$P < 0.05$) (Fig. 10A, B).

Discussion

Here, we declared for the first time that hAD-MSCs can be converted to *Sox1*^{high}/*Nestin*^{high} adNSCs with high purity after cultured successively in the pre-inducing medium, N2B27 medium, and N2B27 medium supplemented with bFGF and EGF. More than 95% cells in adNSCs expressed NSCs markers. The mRNA expression of genes that were associated with embryonic neural development or neural differentiation all increased in the differentiation phase. These *Sox1*^{high}/*Nestin*^{high} NSCs can form neurospheres and have multilineage potential to differentiate into functional neurons, astrocytes, and oligodendrocytes. All these results

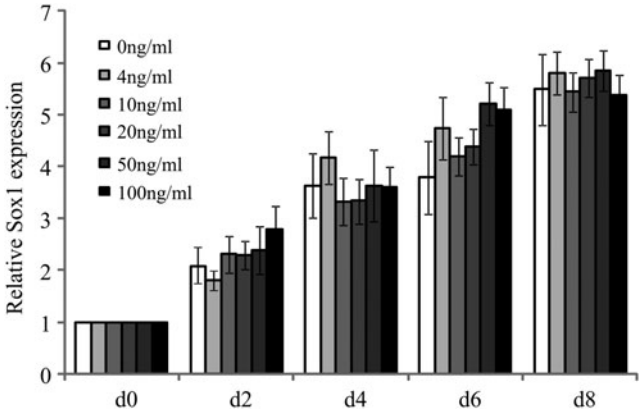

FIG. 8. mRNA expression of *Sox1* in cells cultured in the pre-inducing medium supplemented with different concentrations of bFGF at different time points. There were no differences at same time point between groups with different bFGF concentration.

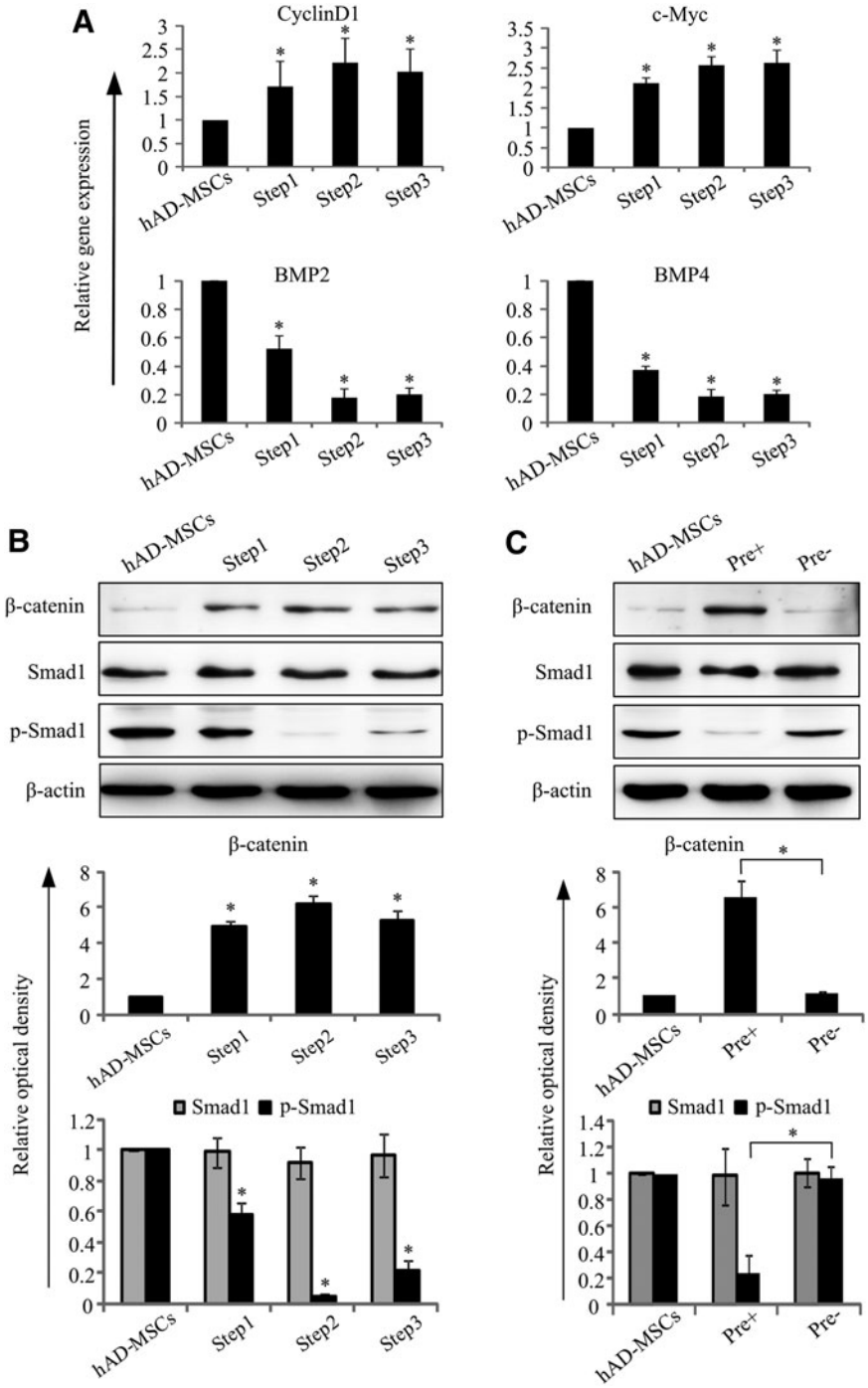

FIG. 9. Activation state of *Wnt/β-catenin* and bone morphogenetic protein (*BMP*) signal pathways in differentiating process. **(A)** Expression of genes related with *Wnt/β-catenin* (*Cyclin D1* and *c-Myc*) and *BMP* (*BMP2* and *BMP4*) signal pathways during differentiation (*$P<0.05$ compared with hAD-MSCs, $n=3$). **(B)** Western blot analysis of *β-catenin*, *Smad1*, and *p-Smad1*, optical density of each band was analyzed. Results showed that protein level of *β-catenin* increased while *p-Smad1* decreased after differentiation (*$P<0.05$ compared with hAD-MSCs, $n=3$). **(C)** Comparison of *Wnt/β-catenin* and *BMP* signal pathways in cells finally obtained in the pre^+ group and pre^- group by western blot. Protein level of *β-catenin* and *p-Smad1* significantly decreased compared with the pre^- group (*$P<0.05$, $n=3$).

indicated that adNSCs we obtained have similar properties with the NSCs from CNS or ESCs [34–37].

As mentioned above, some scientists have got $Nestin^+$ cells from hAD-MSCs. However, Zuk et al. declared that *Nestin* had been found to express in myogenic cells, endothelial cells, and hepatic cells, indicating that *Nestin* expression only is not suitable for the identification of NSCs, especially when there was no functional analysis [26,38]. During embryogenesis, nervous system is originated from neural plate consisted by $Pax6^+/Sox1^-$ neuroepithelium; then, neural plate begins to fold and fuses to form complete neural tube, which consists by $Pax6^+/Sox1^+$ neuroepithelial cells [27]. Neural tube is the primordium of CNS. So the $Pax6^+/Sox1^+$ neuroepithelial cells, which can differentiated into all kinds of cells in CNS, are considered early NSCs [28,29]. By immunostaining analysis, we found that there exists moderate expression of *Pax6* and *Vimentin* in hAD-MSCs, which implied its neural differentiation potential. After induction, we got adNSCs that highly expressed *Sox1, Pax6, Nestin,* and *Vimentin* and possessed tripotent differentiation ability, indicating that adNSCs we got posessed similar phenotype with $Sox1^+/Pax6^+$ neuroepithelial cells. Additionally, NSC-like cells we obtained were highly purified because more than 95% cells expressed NSC markers

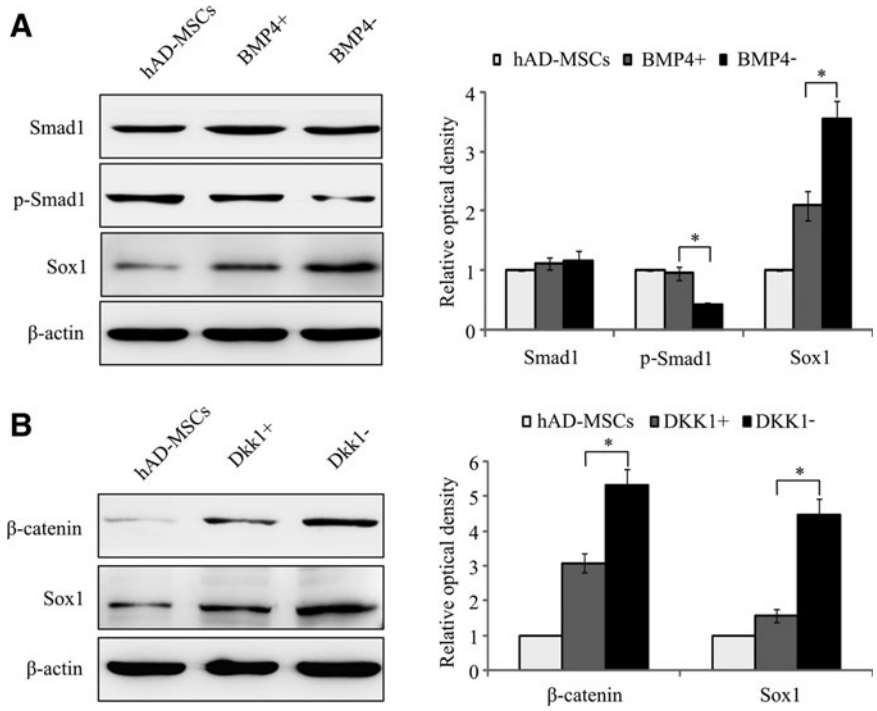

FIG. 10. Expression of *Sox1* was influenced by *BMP* activation ($BMP4^+$) **(A)** and *Wnt/β-catenin* inhibition ($DKK1^+$) **(B)** in pre-inducing process. Expression of *Sox1* was suppressed after treated with BMP4 compared to the BMP^- group or after treated with DKK1 compared to the $DKK1^-$ group ($^*P < 0.05$, $n = 3$).

Sox1, Pax6, Nestin, and *Vimentin*. Moreover, during the inducing process, for every 10^6 hAD-MSCs obtained from the donor, about 5.8×10^8 adNSCs can be obtained, which could be beneficial for the wide application in clinic.

Biological function of seed cells is very important for clinic application. NSC is adult stem cells with tripotent differentiation capability and can differentiate into functional neurons and glia cells [4]. In the present study, the adNSCs possessed tripotent differentiation capability. However, during in vitro inducing process, cells that acquired similar morphological phenotypes with target cells may do not possess biological functions. To generate transplantable NSCs, it is necessary to evaluate neural cells not only by morphology and cells markers but also by its function [32]. Ashjian et al. [39] showed that after induced by a chemical protocol, human adipose-derived stem cells aquired typical neural morphological characteristics and increased expression of neuron specific enolase and *Vimentin*. However, no biological function was detected. As we know, neuron is a kind of excitable cell and is responsible for signal conduction. There exists a variety of ion channels such as sodium, potassium, and calcium ion channels on the membrane of neurons. Influx of sodium ion from extracellular to intracellular through sodium ion channel enables the generation of sodium current, which is the basis of signal transmission. Besides sodium ion channel, during neural development, the number of potassium ion channel increased in mature neurons and low concentration of calcium support the survival and development of neurons [40,41]. In our study, by electrophysiology analysis, we observed the generation of voltage-dependent TTX-sensitive sodium currents in terminal differentiated neurons, which demonstrated the identity of mature neurons. Consistent with electrophysiology data, mRNA expression of sodium ion channel genes *NE-Na* and *SCN5A* were also increased compared to undifferentiated hAD-MSCs, and gene expression associated with potassium and calcium ion channels was also increased, which further indicated the differentiation toward neuronal cells.

Sox1 is a transcriptional factor that belongs to *SoxB1* (Sex determining region Y-box B1) subfamily. Its expression is mainly restricted to neuroectoderm in an activated neural stem/progenitor population [42]. During embryogenesis, it is involved in early development of CNS and the maintenance of neural stem/progenitor cells identity together with *Sox2* and *Sox3*, the other two members of *SoxB1* [43,44]. The onset of *Sox1* is an early response to neural induction signals and correlated with the formation of neural plate [45]. *Sox1*-deficient mice showed behavior disorders and led to epilepsy [46]. In our study, low expression of *Sox1* was detected in hAD-MSCs. After pre-induction, *Sox1* expression was activated and increased significantly in both in mRNA and protein levels. When the expression of *Sox1* was inhibited, the production of adNSCs decreased significantly. Similarly, if pre-inducing step was omitted, the increasing expression of *Sox1* decreased and the NSC differentiation from hAD-MSCs was also suppressed. This demonstrated that *Sox1* was an important factor in this process and pre-inducing step was crucial for the activation of *Sox1*. What's more, *Sox1* exhibited a nuclear translocation process as time extended in the pre-inducing medium, which meant that *Sox1* may function as a transcription factor in this process. That may be the reason why we there existed low neural differentiation in pre^- group. bFGF, the only cytokine in the pre-inducing medium, have no effect on the activation of *Sox1*. Furthermore, we found that *Nestin* expression can be activated in $Sox1^+$ cells in the presence of bFGF and EGF, and very low Nestin was detected when there was low expression of Sox1. In addition, $Sox1^-$ cells cannot transfer to $Nestin^+$ cells despite the presence of bFGF and EGF. These results indicated that Nestin was at the downstream of *Sox1*. This was

consisted with previous report. Tanaka et al. found that group B1 Sox transcription factors, including *Sox1, Sox2* and *Sox3*, could bind with *Nestin* in the neural enhancer and activate its expression [47]. All results showed that the appearance of Nestin and *Sox1* is in line with human CNS development sequence during embryogenesis, that is, *Sox1* activation followed by *Nestin*, which means that the differentiation from hAD-MSCs to adNSCs is a step-by-step process mimicking the neural development. Besides, although gene expression increased, the protein of *Pax6* always located in cytoplasm and we did not observe its nuclear translocation, indicating that *Pax6* did not function as a transcriptional factor during induction.

Cell differentiation can be achieved by many approaches such as treated with chemical reagents [38,48], co-cultured with other cells [49,50], or cultured in the serum-free medium supplemented with cytokines [51,52]. However, cells after treating with chemical reagents were susceptible to death, and the differentiation state was transient and reversible [26,53]; as to co-culture system, cells were easily contaminated and also not suitable for transplantation. Among them, serum-free protocol received more attention because the application of serum-free medium could avoid the contamination of component from animal origin. Cell differentiation can be promoted by sequential addition of cytokines. Thus, initial cells receive continuous stimulation and exhibit stable changes. All medium used in our system were serum-free medium supplemented with/without cytokines, it should be much safer and closer to clinical treatment of neurodegenerative diseases.

Neural development in vivo can be divided into two stages: neural induction (the process from primitive ectoderm to neuroectoderm and form neural plate followed by neural tube. NSCs were induced) and neurogenesis (differentiation of NSCs to terminal neural cells, such as neurons, astrocytes, and oligodendrocytes). In our study, we obtained adNSCs. So this process is similar to neural induction. During embryogenesis, the development of vertebrate is a highly ordered process regulated by multiple signal pathways, so is neural induction. Canonical *Wnt/β-catenin* signaling system is an important pathway in the development of CNS. After treated with a small molecule that activates canonical *WNT* signaling, human ESCs were prone to differentiate into neural progenitors cells under defined conditions [54]. *Wnt/β-catenin* was also involved in the maintenance of NSCs [55]. Here, we found that canonical *Wnt/β-catenin* pathway was greatly activated after pre-inducing process and maintained in the same level in the following steps, whereas the inhibition of *Wnt/β-catenin* pathway influenced *Sox1* expression, indicating that *Wnt/β-catenin* may be involved in this inducing process by *Sox1* regulation.

BMP belongs to the transforming growth factor beta superfamily, and *BMP* signaling is highly conserved in vertebrate and invertebrate. The inhibition of *BMP* signaling is required for the establishment of neuroectoderm. Deleption of *BMP* antagonists such as Chordin blocked the neuroectoderm formation [56]. So noggin, an antagonist of *BMP*, is commonly used in the neural induction from ESCs [57]. Our results showed that *BMP* pathway was partly inhibited after pre-inducing process and totally blocked after cultured in the selection medium. What's more, we also found that BMP signaling was related with *Sox1* expression, which was consistent with the conclusion drawn by larysa that the antagonistic actions of *BMP* signals, and their inhibitors, govern *SoxB1* gene expression (including *Sox1*) in the neuroectoderm [58].

hAD-MSCs can be easily obtained from patients with little pain, so it became one of the most promising cell sources for the treatment of neurodegenerative diseases. A safe induction system from hAD-MSCs to adNSCs is the precondition of clinical application. In the induction protocol we established here, it is no need to add expensive cytokines and the use of serum replacement greatly rules out the occurrence of immune rejection. Highly purified NSCs with uniform properties make the stem cell-based therapy more stable and easier controlled. What's more, it is a very good cell model for drug selection in personalized medicine. However, in vitro induction of hAD-MSCs to NSCs is just the first step, whether adNSCs we obtained have functions in vivo remains unknown and needs further investigation.

Acknowledgments

We are grateful to thank Jimin Cao, Xiaoqiu Tan, and Li Yan for their technical assistant on electrophysiological analysis. This work was supported by grants from the "863 Projects" of the Ministry of Science and Technology of the People's Republic of China (no.2011AA020100), National Natural Science Foundation of China (no. 30830052), the National Key Scientific Program of China (no. 2011CB964901), and Program for Cheung Kong Scholars and Innovative Research Team in University-PCSIRT (NO,IRT0909).

Author Disclosure statement

The authors have no conflicts of interest.

References

1. Feng Z and F Gao. (2012). Stem cell challenges in the treatment of neurodegenerative disease. CNS Neurosci Ther 18:142–148.
2. Brown RC, AH Lockwood and BR Sonawane. (2005). Neurodegenerative diseases: an overview of environmental risk factors. Environ Health Perspect 113:1250–1256.
3. Honig LS and RN Rosenberg. (2000). Apoptosis and neurologic disease. Am J Med 108:317–330.
4. Mujtaba T, DR Piper, A Kalyani, AK Groves, MT Lucero and MS Rao. (1999). Lineage-restricted neural precursors can be isolated from both the mouse neural tube and cultured ES cells. Dev Biol 214:113–127.
5. Riess P, C Zhang, KE Saatman, HL Laurer, LG Longhi, R Raghupathi, PM Lenzlinger, J Lifshitz, J Boockvar, et al. (2002). Transplanted neural stem cells survive, differentiate, and improve neurological motor function after experimental traumatic brain injury. Neurosurgery 51:1043–1052; discussion 1052–1054.
6. Wong AM, H Hodges and K Horsburgh. (2005). Neural stem cell grafts reduce the extent of neuronal damage in a mouse model of global ischaemia. Brain Res 1063:140–150.
7. Ben-Hur T, RB van Heeswijk, O Einstein, M Aharonowiz, R Xue, EE Frost, S Mori, BE Reubinoff and JW Bulte. (2007). Serial *in vivo* MR tracking of magnetically labeled neural spheres transplanted in chronic EAE mice. Magn Reson Med 57:164–171.
8. Einstein O, N Fainstein, I Vaknin, R Mizrachi-Kol, E Reihartz, N Grigoriadis, I Lavon, M Baniyash, H Lassmann

and T Ben-Hur. (2007). Neural precursors attenuate autoimmune encephalomyelitis by peripheral immunosuppression. Ann Neurol 61:209–218.
9. Einstein O, N Grigoriadis, R Mizrachi-Kol, E Reinhartz, E Polyzoidou, I Lavon, I Milonas, D Karussis, O Abramsky and T Ben-Hur. (2006). Transplanted neural precursor cells reduce brain inflammation to attenuate chronic experimental autoimmune encephalomyelitis. Exp Neurol 198:275–284.
10. Einstein O, D Karussis, N Grigoriadis, R Mizrachi-Kol, E Reinhartz, O Abramsky and T Ben-Hur. (2003). Intraventricular transplantation of neural precursor cell spheres attenuates acute experimental allergic encephalomyelitis. Mol Cell Neurosci 24:1074–1082.
11. Ben-Hur T, O Einstein, R Mizrachi-Kol, O Ben-Menachem, E Reinhartz, D Karussis and O Abramsky. (2003). Transplanted multipotential neural precursor cells migrate into the inflamed white matter in response to experimental autoimmune encephalomyelitis. Glia 41:73–80.
12. Pluchino S, A Quattrini, E Brambilla, A Gritti, G Salani, G Dina, R Galli, CU Del, S Amadio, et al. (2003). Injection of adult neurospheres induces recovery in a chronic model of multiple sclerosis. Nature 422:688–694.
13. Pluchino S, L Zanotti, B Rossi, E Brambilla, L Ottoboni, G Salani, M Martinello, A Cattalini, A Bergami, et al. (2005). Neurosphere-derived multipotent precursors promote neuroprotection by an immunomodulatory mechanism. Nature 436:266–271.
14. Hallbergson AF, C Gnatenco and DA Peterson. (2003). Neurogenesis and brain injury: managing a renewable resource for repair. J Clin Invest 112:1128–1133.
15. Taghipour M and A Razmkon. (2012). Isolation and growth of neural stem cells derived from adult human hippocampus. J Inj Violence Res 4.
16. Sun Y, S Pollard, L Conti, M Toselli, G Biella, G Parkin, L Willatt, A Falk, E Cattaneo and A Smith. (2008). Long-term tripotent differentiation capacity of human neural stem (NS) cells in adherent culture. Mol Cell Neurosci 38:245–258.
17. Koch P, T Opitz, JA Steinbeck, J Ladewig and O Brustle. (2009). A rosette-type, self-renewing human ES cell-derived neural stem cell with potential for *in vitro* instruction and synaptic integration. Proc Natl Acad Sci U S A 106:3225–3230.
18. Salewski RP, J Buttigieg, RA Mitchell, D van der Kooy, A Nagy and MG Fehlings. (2013). The generation of definitive neural stem cells from PiggyBac transposon-induced pluripotent stem cells can be enhanced by induction of the NOTCH signaling pathway. Stem Cells Dev 22:383–396.
19. Friedenstein AJ, RK Chailakhyan, NV Latsinik, AF Panasyuk and IV Keiliss-Borok. (1974). Stromal cells responsible for transferring the microenvironment of the hemopoietic tissues. Cloning *in vitro* and retransplantation *in vivo*. Transplantation 17:331–340.
20. Aust L, B Devlin, SJ Foster, YD Halvorsen, K Hicok, T du Laney, A Sen, GD Willingmyre and JM Gimble. (2004). Yield of human adipose-derived adult stem cells from liposuction aspirates. Cytotherapy 6:7–14.
21. Takemitsu H, D Zhao, I Yamamoto, Y Harada, M Michishita and T Arai. (2012). Comparison of bone marrow and adipose tissue-derived canine mesenchymal stem cells. BMC Vet Res 8:150.
22. Zhu X, J Du and G Liu. (2012). The comparison of multilineage differentiation of bone marrow and adipose-derived mesenchymal stem cells. Clin Lab 58:897–903.
23. Nakagami H, R Morishita, K Maeda, Y Kikuchi, T Ogihara and Y Kaneda. (2006). Adipose tissue-derived stromal cells as a novel option for regenerative cell therapy. J Atheroscler Thromb 13:77–81.
24. Ikegame Y, K Yamashita, S Hayashi, H Mizuno, M Tawada, F You, K Yamada, Y Tanaka, Y Egashira, et al. (2011). Comparison of mesenchymal stem cells from adipose tissue and bone marrow for ischemic stroke therapy. Cytotherapy 13:675–685.
25. Hsueh YY, YL Chiang, CC Wu and SC Lin. (2012). Spheroid formation and neural induction in human adipose-derived stem cells on a chitosan-coated surface. Cells Tissues Organs 196:117–128.
26. Ahmadi N, S Razavi, M Kazemi and S Oryan. (2012). Stability of neural differentiation in human adipose derived stem cells by two induction protocols. Tissue Cell 44:87–94.
27. Zhang SC. (2006). Neural subtype specification from embryonic stem cells. Brain Pathol 16:132–142.
28. Li XJ, ZW Du, ED Zarnowska, M Pankratz, LO Hansen, RA Pearce and SC Zhang. (2005). Specification of motoneurons from human embryonic stem cells. Nat Biotechnol 23:215–221.
29. Pankratz MT, XJ Li, TM Lavaute, EA Lyons, X Chen and SC Zhang. (2007). Directed neural differentiation of human embryonic stem cells via an obligated primitive anterior stage. Stem Cells 25:1511–1520.
30. Li K, Q Han, X Yan, L Liao and RC Zhao. (2010). Not a process of simple vicariousness, the differentiation of human adipose-derived mesenchymal stem cells to renal tubular epithelial cells plays an important role in acute kidney injury repairing. Stem Cells Dev 19:1267–1275.
31. Hermann A, R Gastl, S Liebau, MO Popa, J Fiedler, BO Boehm, M Maisel, H Lerche, J Schwarz, R Brenner and A Storch. (2004). Efficient generation of neural stem cell-like cells from adult human bone marrow stromal cells. J Cell Sci 117:4411–4422.
32. Jang S, HH Cho, YB Cho, JS Park and HS Jeong. (2010). Functional neural differentiation of human adipose tissue-derived stem cells using bFGF and forskolin. BMC Cell Biol 11:25.
33. Chiba S, MS Kurokawa, H Yoshikawa, R Ikeda, M Takeno, M Tadokoro, H Sekino, T Hashimoto and N Suzuki. (2005). Noggin and basic FGF were implicated in forebrain fate and caudal fate, respectively, of the neural tube-like structures emerging in mouse ES cell culture. Exp Brain Res 163:86–99.
34. Liang P, S Zhao, K Kawamoto, L Jin and E Liu. (2003). Neuronal and glial differentiation following culture of the human embryonic cortical stem cells. Hum Cell 16:151–156.
35. Joo KM, BG Kang, JY Yeon, YJ Cho, JY An, HS Song, JH Won, SJ Kim, SC Hong and DH Nam. (2013). Experimental and clinical factors influencing long-term stable *in vitro* expansion of multipotent neural cells from human adult temporal lobes. Exp Neurol 240:168–177.
36. Zhao J, W Sun, HM Cho, H Ouyang, W Li, Y Lin, J Do, L Zhang, S Ding, et al. (2013). Integration and long distance axonal regeneration in the central nervous system from transplanted primitive neural stem cells. J Biol Chem 288:164–168.
37. Elkabetz Y, G Panagiotakos, SG Al, ND Socci, V Tabar and L Studer. (2008). Human ES cell-derived neural rosettes reveal a functionally distinct early neural stem cell stage. Genes Dev 22:152–165.
38. Zuk PA, M Zhu, P Ashjian, DA De Ugarte, JI Huang, H Mizuno, ZC Alfonso, JK Fraser, P Benhaim and MH Hedrick. (2002). Human adipose tissue is a source of multipotent stem cells. Mol Biol Cell 13:4279–4295.
39. Ashjian PH, AS Elbarbary, B Edmonds, D DeUgarte, M Zhu, PA Zuk, HP Lorenz, P Benhaim and MH Hedrick. (2003).

In vitro differentiation of human processed lipoaspirate cells into early neural progenitors. Plast Reconstr Surg 111:1922–1931.
40. Richter H, R Klee, U Heinemann and C Eder. (1997). Developmental changes of inward rectifier currents in neurons of the rat entorhinal cortex. Neurosci Lett 228:139–141.
41. Furlan F, L Guasti, D Avossa, A Becchetti, E Cilia, L Ballerini and A Arcangeli. (2005). Interneurons transiently express the ERG K+ channels during development of mouse spinal networks *in vitro*. Neuroscience 135:1179–1192.
42. Venere M, YG Han, R Bell, JS Song, A Alvarez-Buylla and R Blelloch. (2012). Sox1 marks an activated neural stem/progenitor cell in the hippocampus. Development 139:3938–3949.
43. Guth SI and M Wegner. (2008). Having it both ways: Sox protein function between conservation and innovation. Cell Mol Life Sci 65:3000–3018.
44. Nitta KR, S Takahashi, Y Haramoto, M Fukuda, Y Onuma and M Asashima. (2006). Expression of Sox1 during Xenopus early embryogenesis. Biochem Biophys Res Commun 351:287–293.
45. Pevny LH, S Sockanathan, M Placzek and R Lovell-Badge. (1998). A role for SOX1 in neural determination. Development 125:1967–1978.
46. Malas S, M Postlethwaite, A Ekonomou, B Whalley, S Nishiguchi, H Wood, B Meldrum, A Constanti and V Episkopou. (2003). Sox1-deficient mice suffer from epilepsy associated with abnormal ventral forebrain development and olfactory cortex hyperexcitability. Neuroscience 119:421–432.
47. Tanaka S, Y Kamachi, A Tanouchi, H Hamada, N Jing and H Kondoh. (2004). Interplay of SOX and POU factors in regulation of the Nestin gene in neural primordial cells. Mol Cell Biol 24:8834–8846.
48. Ou Y, XD Yuan, YN Cai and YH Lu. (2011). Ultrastructure and electrophysiology of astrocytes differentiated from adult adipose-derived stromal cells. Chin Med J (Engl) 124:2656–2660.
49. Liao D, P Gong, X Li, Z Tan and Q Yuan. (2010). Co-culture with Schwann cells is an effective way for adipose-derived stem cells neural transdifferentiation. Arch Med Sci 6:145–151.
50. Wang B, J Han, Y Gao, Z Xiao, B Chen, X Wang, W Zhao and J Dai. (2007). The differentiation of rat adipose-derived stem cells into OEC-like cells on collagen scaffolds by co-culturing with OECs. Neurosci Lett 421:191–196.
51. Chen J, YX Tang, YM Liu, J Chen, XQ Hu, N Liu, SX Wang, Y Zhang, WG Zeng, et al. (2012). Transplantation of adipose-derived stem cells is associated with neural differentiation and functional improvement in a rat model of intracerebral hemorrhage. CNS Neurosci Ther 18:847–854.
52. Zavan B, L Michelotto, L Lancerotto, PA Della, D D'Avella, G Abatangelo, V Vindigni and R Cortivo. (2010). Neural potential of a stem cell population in the adipose and cutaneous tissues. Neurol Res 32:47–54.
53. Qian DX, HT Zhang, X Ma, XD Jiang and RX Xu. (2010). Comparison of the efficiencies of three neural induction protocols in human adipose stromal cells. Neurochem Res 35:572–579.
54. Kirkeby A, S Grealish, DA Wolf, J Nelander, J Wood, M Lundblad, O Lindvall and M Parmar. (2012). Generation of regionally specified neural progenitors and functional neurons from human embryonic stem cells under defined conditions. Cell Rep 1:703–714.
55. Chenn A and CA Walsh. (2002). Regulation of cerebral cortical size by control of cell cycle exit in neural precursors. Science 297:365–369.
56. Oelgeschlager M, H Kuroda, B Reversade and EM De Robertis. (2003). Chordin is required for the Spemann organizer transplantation phenomenon in Xenopus embryos. Dev Cell 4:219–230.
57. Gerrard L, L Rodgers and W Cui. (2005). Differentiation of human embryonic stem cells to neural lineages in adherent culture by blocking bone morphogenetic protein signaling. Stem Cells 23:1234–1241.
58. Pevny L and M Placzek. (2005). SOX genes and neural progenitor identity. Curr Opin Neurobiol 15:7–13.

Address correspondence to:
Dr. Robert Chunhua Zhao
Center of Excellence in Tissue Engineering
Chinese Academy of Medical Sciences
and Peking Union Medical College
Institute of Basic Medical Sciences and School of Basic Medicine
5# Dongdansantiao
Beijing 100005
People's Republic of China

E-mail: chunhuaz@public.tpt.tj.cn

Received for publication June 9, 2013
Accepted after revision October 18, 2013
Prepublished on Liebert Instant Online October 18, 2013